Available online at www.sciencedirect.com
SCIENCE DIRECT®
Journal of Crystal Growth 253 (2003) 71–76
JOURNAL OF CRYSTAL GROWTH
www.elsevier.com/locate/jcrysgro

Modified droplet epitaxy GaAs/AlGaAs quantum dots grown on a variable thickness wetting layer

S. Sanguinetti[a,b,*], K. Watanabe[b], T. Tateno[b], M. Gurioli[a,c], P. Werner[d], M. Wakaki[e], N. Koguchi[b]

[a] *I.N.F.M. Dipartimento di Scienza dei Materiali, Università di Milano Bicocca, Via Cozzi 53, I-20125 Milano, Italy*
[b] *National Institute for Materials Science, 1–2–1 Sengen, Tsukuba, Ibaraki 305–0047, Japan*
[c] *L.E.N.S., Via Sansone 1, I-50019 Sesto Fiorentino, Italy*
[d] *Max-Planck-Institut für Mikrostrukturphysik, Weinberg 2, D-06120 Halle, Germany*
[e] *Department of Electro-Photo Optics, Tokai University, Hiratsuka, Kanagawa 259-1292, Japan*

Received 7 February 2003; accepted 14 February 2003
Communicated by M. Schieber

Abstract

We show that the use of modified droplet epitaxy allows to tune the wetting layer thickness in GaAs quantum dot structures. Morphological observations demonstrate that the wetting layer at the base of the dots can be controlled or even removed by changing the surface stoichiometry of substrates before droplet formations. Spectroscopical measurements show that the variation of the wetting layer thickness strongly influences the optical properties of the dots. The experimental transition energies of the dots well agree with a theoretical model based on effective mass approximation.

PACS: 78.67.Hc; 68.35.Fx

Keywords: A3. Molecular beam epitaxy; A3. Quantum dots; B2. Semiconducting III–V materials

1. Introduction

The discovery of the self–organized growth of high quality semiconductor quantum dots (QD), obtained by droplet epitaxy [1–3] or, more commonly, via strained epilayer epitaxy in the Stranski–Krastanov (SK) growth mode [4,5], has triggered an in-depth research of the physical phenomena related to the QD growth. New paths for obtaining QDs with novel physical properties, which may give devices with even higher performances, are therefore of the utmost relevance [6]. Lately, we reported on a modified droplet epitaxy (MDE) method for self–assembling high density, strain free and defect free QDs [7]. The MDE growth method does not require the lattice mismatch constraint as in the SK method and therefore permits the growth of QDs whose

*Corresponding author. I.N.F.M. Dipartimento di Scienza dei Materiali, Università di Milano Bicocca, Via Cozzi 53, I-20125 Milano, Italy. Tel.: +39-02-6448-5156; Fax: +39-02-6448-5400.
E-mail address: stefano.sanguinetti@unimib.it (S. Sanguinetti).

0022-0248/03/$ - see front matter
doi:10.1016/S0022-0248(03)01016-9

composition is completely uncorrelated with that of the growth substrate. The QD samples grown with this methodology (GaAs/AlGaAs) show a good emission yield, even at room temperature [7,8].

A further peculiarity of the SK growth is the unavoidable presence of bidimensional layer, or wetting layer (WL), of the same material of the dots, which mediates the electronic interaction between the barrier states and the localized QD states. The presence of a bidimensional layer connecting the QDs has strong influences on the optical properties and carrier kinetics of the QDs. Let us only mention, the increasing attention that recently has been devoted to the exact role of the WL in the carrier relaxation and thermalization in SK self–assembled QD systems [9–15]. At the same time, in the SK growth the thickness of the WL only depends on the lattice mismatch between the substrate and the QD layer and cannot be controlled.

The relaxation of the lattice mismatch constraint in the MDE allows to explore further novel types of QD structures. Here we report on the fabrication of GaAs/$Al_{0.3}Ga_{0.7}As$ QDs without any wetting layer in the structure, or, on the other side, a quantum well of the same material of the dots can be inserted at the base of the QD thus acting as a WL of controlled thickness. A detailed morphological and optical characterization of the QD materials is also shown. The QD optical transition nicely agrees with the prediction of an effective mass model.

2. Sample growth and experimental details

All the samples were grown by Riber-32 P molecular beam epitaxy (MBE) system on semi–insulating GaAs (0 0 1) wafers. The sample structures start with the deposition, at 580°C, of a 300 nm thick GaAs buffer followed by a 500 nm $Al_{0.3}Ga_{0.7}As$ barrier layer. At this point, the growth sequence is differentiated depending on the presence or not, in the sample design, of a variable thickness WL.

The QD sample without WL (sample A) is realized as follows. After the growth of $Al_{0.3}Ga_{0.7}As$ barrier layer, the substrate temperature is reduced to 180°C, the As valve closed and the As pressure in the growth chamber depleted. In these conditions, an arsenic terminated surface in the c(4 × 4) reconstruction is observed via reflection high-energy electron diffraction (RHEED). Because group III metal droplets are not formed on the As–stabilized surfaces but rather on group III stabilized surfaces, 1.75 monolayers (ML) of $Al_{0.3}Ga_{0.7}$ are supplied in order to saturate the 1.75 MLs excess As atoms present on the c(4 × 4) surface. This results in the appearance of a group III $Al_{0.3}Ga_{0.7}As$ stabilized surface. The growth sequence continues with the deposition of 3.0 MLs of Ga in order to form the Ga droplets.

The QD samples with variable thickness WL connecting the dots are realized as follows. After the growth of the $Al_{0.3}Ga_{0.7}As$ barrier layer, n MLs of GaAs are deposited at 580°C. Then the substrate temperature is reduced to 180°C and the arsenic depleted from the growth chamber. At this point, 4.75 MLs of Ga are supplied to c(4 × 4) surface. The initial 1.75 MLs of Ga are incorporated in the As rich surface in order to produce the group III stabilized surface necessary for the formation of the Ga droplet. The $n+1.75$MLs of GaAs constitute the WL; the remaining 3MLs of Ga form the droplet. Two different WL thickness were grown: $n = 1.25$ MLs (sample B) and $n =$ 6.25 MLs (sample C).

After the Ga droplets formation, an As^4 molecular beam is irradiated on the sample for the crystallization of the droplet maintaining the substrate temperature at 180°C. The change from a halo to a spotty RHEED pattern shows the onset of the three–dimensional growth mode. The detailed mechanism of the QD formation by MDE can be found in Ref. [7]. A 10 nm thick $Al_{0.3}Ga_{0.7}As$ overlayer is grown by migration enhanced epitaxy (MEE) at the same 180°C temperature in order to prevent two–dimensional regrowth of the naked GaAs microcrystals [7]. Then, the growth temperature was raised back to 580°C and samples were annealed for 10 min with As^4 flux. A capping layer of 90 nm of $Al_{0.3}Ga_{0.7}As$ is grown by ordinary MBE. After that, the samples are annealed at 600°C in As^4 atmosphere for 60 min in order to improve the QD quality.

Finally, the structure is terminated with 10 nm thick GaAs cap layer grown at 580°C. Two quantum wells of 8MLs and 3MLs thickness, obtained by depositing only 1.75 MLs of Ga, thus avoiding droplet formation during the growth, were also realized as reference samples.

The surface morphologies and cross–sections of the samples were observed by field-emission type high-resolution scanning electron microscopy (HRSEM) and by transmission electron microscopy (TEM). For the latter case, plan-view samples as well as cross-section samples were prepared by conventional techniques including ion-milling. For the conventional diffraction contrast imaging an Philips CM 20 transmission microscope was used (acceleration voltage 200 kV), for the high-resolution electron microscopy (HREM) an JEOL JEM 4010 (400 kV). Image processing was partly applied for HREM micrographs to analyze the crystal lattice structure.

CW photoluminescence (PL) spectra were measured at 20 K. The PL was excited with an Ar^+ laser in multiline mode. The excitation power density P_{exc} ranged from 0.5 to 5000 W/cm^2, with a spot diameter of 500 or 100 μm. PL spectra were measured by a grating monochromator operating with a GaAs photomultiplier.

3. Results and discussion

Fig. 1 shows the typical surface morphology of the GaAs QDs before the overlayer growth, obtained by HREM. The dot density was 3.0×10^{10} cm^{-2}, with a mean diameter of ≈20 nm. The corresponding cross-section TEM micrographs are presented in Fig. 2. Due to the bright–field imaging conditions chosen, the islands as well as the wetting layer would be presented by a darker contrast. The brighter surrounding fringes relate to strain fields in the matrix. All the samples A, B and C show the presence of QD with comparable size and density. The WL connecting the dots, however, could only be observed in the two samples B and C (Fig. 2b and c and Fig. 3b),

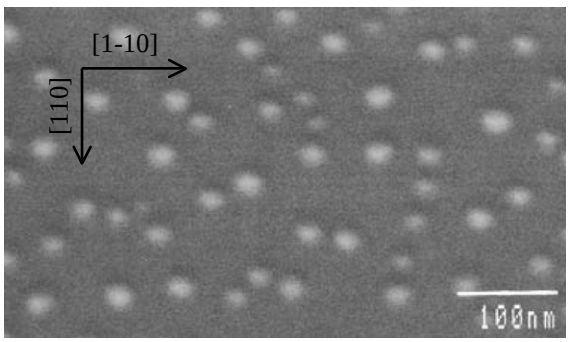

Fig. 1. Surface HREM image of an uncapped QD sample.

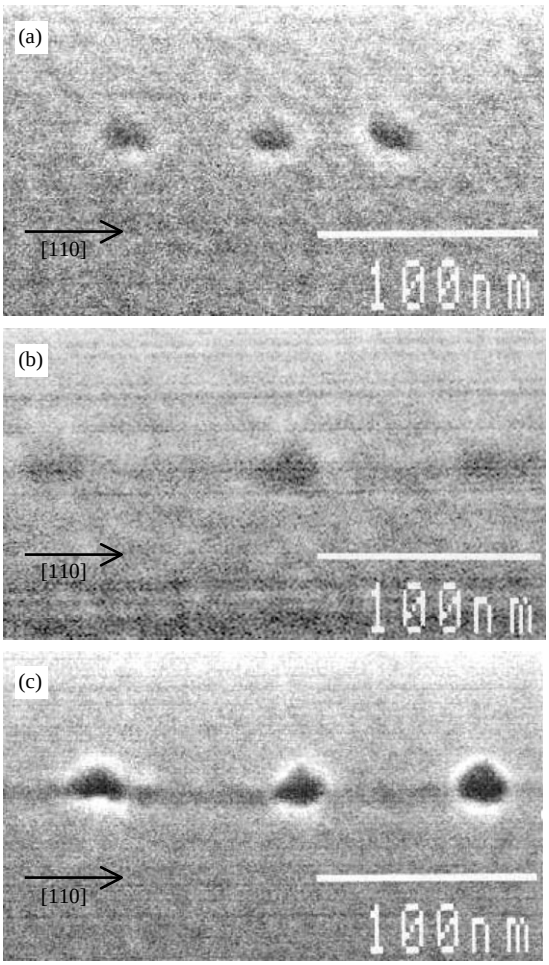

Fig. 2. Cross-section TEM micrographs, taken along the [1 1 1] axis: (a) QDs without WL; (b) QDs with 3 MLs WL; and (c) QDs with 8 MLs WL. In such bright-field images QD as well as the WL appear with a darker contrast.

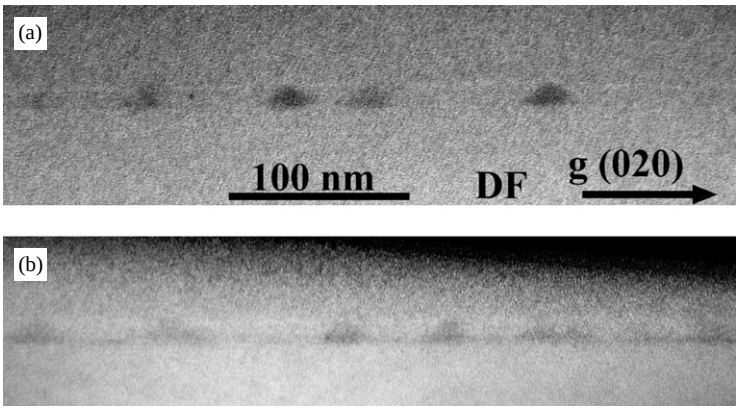

Fig. 3. Cross-section TEM images, taken along the [0 2 0] axis: (a) sample A: QDs without WL; and (b) sample B: QD with 3 MLs WL.

which were expressly grown with 3MLs and 8MLs WL. The HREM and TEM images of sample A (Fig. 2a and Fig. 3a), on the other side, confirm the lack of the WL in this layer structure.

Low temperature (20 K) PL spectra of the three QD samples are reported in Fig. 4. All the samples show a strong and broad PL band attributed to QD emission. The QD emission red–shifts with the thickness of the underlying WL, being 1.67, 1.65 and 1.60 eV for samples A, B and C, respectively. The PL full-width at half-maximum (FWHM) is $\approx$100 meV for samples A and B. Sample C shows a much narrower emission, with a FWHM of 60 meV. The emission from the QW reference samples (not shown here) is centered at 1.76 eV for the 8 MLs QW and 1.89 eV for the 3 MLs QW, respectively.

Increasing the excitation power density (P_{exc}) in the 0.5–5000 W/cm^2 range, produces a clear band filling effect, as displayed in Fig. 5. While the ground state emission tends to saturate, a high–energy shoulder is superlinearly growing with P_{exc}. We attribute this emissions to excited state recombination. The excited state energies are 1.74, 1.73 and 1.67 eV in the samples A, B and C, respectively. All the samples show a superlinear dependence of the QD PL integrated intensity with respect to P_{exc}. In sample C an additional line is appearing at high P_{exc} at 1.76 eV. We attribute this emission to the 8 MLs WL emission, due to the close coincidence of the emission energy with that of the reference QW. WL emission has not been detected in sample B.

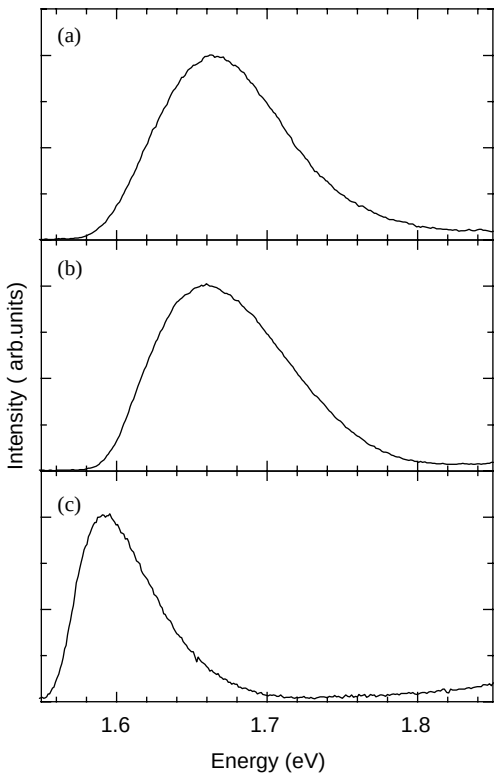

Fig. 4. Low temperature (20 K) PL spectra of the samples A (a), B (b) and C (c). The excitation power density was 5 W/cm^2.

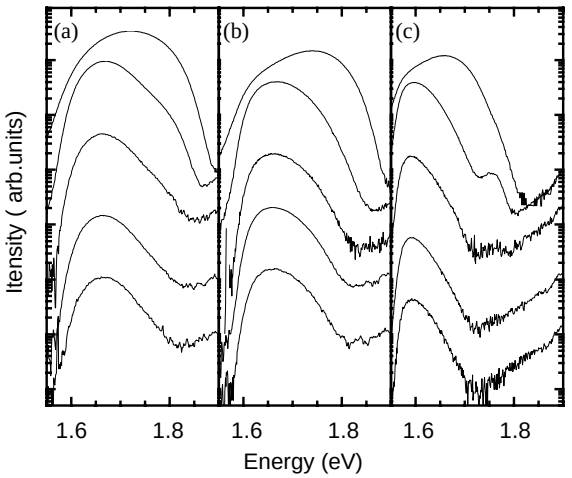

Fig. 5. Five different PL spectra taken at increasing excitation power densities at steps of one optical density in the range $0.5\,W/cm^2$– $5\,kW/cm^2$ of the samples A (a), B (b) and C (c). All the measurements were performed at $T = 20\,K$.

The observed QD emission red–shift with the increasing WL thickness should stem from the larger volume available to the QD electronic wave function when a WL of sizeable thickness is present at the base of the QD. In sample C the presence of the 6.25 MLs WL nearly doubles the effective volume available to the QD electronic wave functions with respect to QDs grown without WL. As a matter of fact the confinement energy—given by the difference of the QD PL energy and the GaAs band gap—is almost doubled in the sample A with respect to sample C. Also the observed reduction of the PL FWHM is due to the reduction of the carrier confinement energy in the QD with WL. Similar size fluctuation of the droplet islands gives rise to a minor spread of the QD fundamental optical transition when the confinement energy is largely reduced.

In order to check quantitatively these considerations we have performed the calculation of the QD electronic structure of the realistic structure within the effective mass approximation, following the method outlined in Ref. [16]. The dot shape, pyramidal, has been approximated by cone with the same height and base (base size of ≈ 20 nm and height of ≈ 16 nm). The WLs of 3 MLs (1.25MLs MBE + 1.75 MLs MDE) and 8 MLs (6.25 MLs MBE + 1.75 MLs MDE) were introduced in the structure of samples B and C, respectively. The material parameters used in the calculation are reported in Table 1 of Ref. [8].

Care has been devoted to the correct description of the annealing effects on the heterostructures. It is worth noting that the $Al_{0.3}Ga_{0.7}As$ WL, when present, is the result of two different growth steps: a standard MBE step, where n MLs are grown at 580°C, and an MDE step, where 1.75 MLs GaAs are generated due to the incorporation of Ga at low temperature (180°C) in the As terminated $c(4 \times 4)$ surface. Ga and Al interdiffusion in MBE grown GaAs/AlGaAs hetero–interfaces becomes relevant only for temperatures above 800°C [17], while important interdiffusion (≈ 1 nm) has been observed in MDE materials even at 520°C [8]. The thin 1.75 MLs of GaAs resulting from Ga incorporation at low temperature is washed out after 60 min annealing at 600°C [8]. We therefore expect that, after the annealing step, only the MBE grown part of the WL would remain with relatively sharp hetero–interfaces, modified in the growth direction by the exponentially decreasing tail of excess Ga resulting from the diffusion of the MDE material. This process has been taken into account by calculating the changes in the potential profile of the dot induced by the group III interdiffusion processes during the annealing procedure in MDE–QDs [8]. The best reproduction of sample A ground and excited state energies are obtained allowing for 1.3 nm diffusion length, in good agreement with what observed in MDE–QD materials subjected to similar annealing process (≈ 1.5 nm [8]). The electronic structures of sample B and C were calculated by allowing for 1.3 nm diffusion length for the MDE material. Interdiffusion of the MBE layers have been neglected due to the very low annealing temperature.

The results for the relevant optical transitions are reported in Fig. 6 for different values of the MBE WL thickness and compared with the experimental data. A nice agreement between the predicted and observed transition energies is found demonstrating the strong influence of the WL on the optical properties of the QDs.

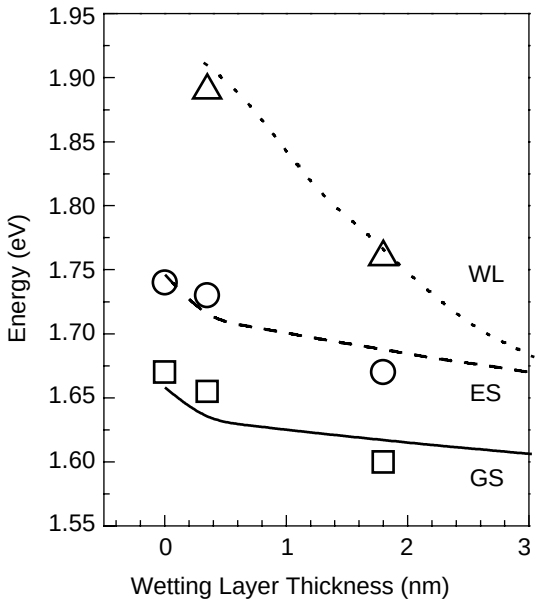

Fig. 6. Comparison between experimental and calculated transition energies of the wetting layer (triangles and dotted line) and the ground state (squares and continuous line) and the excited state (circles and dashed lines) of the QD.

4. Conclusions

The MDE growth procedure offers additional degree of freedom in the band gap engineering of the QD materials. We shown that, GaAs QDs without WL were successfully fabricated by droplet epitaxy with changing surface stoichiometry of substrates before droplet deposition. QD structures containing WL with controlled thickness were also grown by droplet formation on GaAs QWs of different width. The QD optical properties are modified by the WL presence, in good agreement with the theoretical predictions. We believe that this class of materials should be of the utmost importance for a deeper understanding of the role of the WL in the optical properties, carrier dynamics, carrier thermal distribution and PL quenching in QD materials.

References

[1] N. Koguchi, S. Takahashi, T. Chikyow, J. Crystal Growth 111 (1991) 688.
[2] N. Koguchi, K. Ishige, Jpn. J. Appl. Phys. 32 (1993) 2052.
[3] N. Koguchi, K. Ishige, S. Takahashi, J. Vac. Sci. Technol. B 11 (1993) 787.
[4] D. Bimberg, M. Grundmann, N.N. Ledentsov, Quantum Dots Heterostructures, Wiley, New York, 1999.
[5] L. Goldstein, F. Glas, J.Y. Marzin, M.N. Charasse, G. LeRoux, Appl. Phys. Lett. 47 (1985) 1099.
[6] N.N. Ledentsov, V.A. Shchukin, M. Grundmann, N. Kirstaedter, J. Böhrer, O. Schmidt, D. Bimberg, V.M. Ustinov, A.Y. Egorov, A.E. Zhukov, et al., Phys. Rev. B 54 (1996) 8743.
[7] K. Watanabe, N. Koguchi, Y. Gotoh, Jpn. J. Appl. Phys. 39 (2000) L79.
[8] S. Sanguinetti, K. Watanabe, T. Kuroda, F. Minami, Y. Gotoh, N. Koguchi, J. Crystal Growth 242 (2002) 321.
[9] Y. Yoda, O. Moriwaki, M. Nishioka, Y. Arakawa, Phys. Rev. Lett. 82 (1999) 4114.
[10] D. Morris, N. Perret, S. Fafard, Appl. Phys. Lett. 75 (1999) 3593.
[11] A.V. Uskov, J. McInerney, F. Adler, H. Schweizer, M.H. Pilkuhn, Appl. Phys. Lett. 72 (1998) 58.
[12] S. Raymond, K. Hinzer, S. Fafard, J.L. Merz, Phys. Rev. B 61 (2000) 16331.
[13] L. Brusaferri, S. Sanguinetti, E. Grilli, M. Guzzi, A. Bignazzi, F. Bogani, L. Carraresi, M. Colocci, A. Bosacchi, P. Frigeri, et al., Appl. Phys. Lett. 69 (1996) 3354.
[14] W. Yang, R.R. Lowe-Webb, H. Lee, P.C. Sercel, Phys. Rev. B 56 (1997) 13314.
[15] S. Sanguinetti, M. Henini, M. Grassi-Alessi, M. Capizzi, P. Frigeri, S. Franchi, Phys. Rev. B 60 (1999) 8276.
[16] J.Y. Marzin, G. Bastard, Solid State Commun. 92 (1994) 437.
[17] T.E. Schlesinger, T. Kuech, Appl. Phys. Lett. 49 (1986) 519.